

## Article

# Bamboo Structure and Its Impact on Mechanical Properties: A Case Study of *Bambusa arundinaceae*

Kangjian Zhang<sup>1,2,3,†</sup>, Linpeng Yu<sup>1,2,3,†</sup>, Fukuan Dai<sup>1,2</sup>, Yuxuan Chen<sup>1,2</sup>, Zehui Jiang<sup>1,2</sup>, Youhong Wang<sup>3</sup> and Genlin Tian<sup>1,2,\*</sup>

<sup>1</sup> Institute of New Bamboo and Rattan Based Biomaterials, International Center for Bamboo and Rattan, Beijing 100102, China

<sup>2</sup> Key Laboratory of National Forestry and Grassland Administration/Beijing for Bamboo & Rattan Science and Technology, Beijing 100102, China

<sup>3</sup> School of Materials and Chemistry, Anhui Agricultural University, Hefei 230036, China

\* Correspondence: tiangenlin@icbr.ac.cn; Tel.: +86-010-84789817

† These authors contributed equally to this work.

**Abstract:** Bamboo is a naturally occurring composite material, which exhibits a decomposable structure with varying composition. The distinct structural features of bamboo contribute to its exceptional strength and flexibility, making it an excellent choice for construction purposes. However, only a limited portion of bamboo species has been studied for its mechanical properties, and research on *Bambusa arundinaceae* has primarily focused on its pharmaceutical values. Therefore, we investigated the relationship between the structural characteristics of *B. arundinaceae* and its mechanical properties using axial compression experiments and tangential bending experiments. The results showed that the distribution density of vascular bundles (VBs) of *B. arundinaceae* ranged from 1.98 to 4.34 pcs/mm<sup>2</sup>, while the volume fraction of fiber sheaths (FSs) ranged from 35.82 to 42.58%. The average compressive strength, flexural strength, and flexural elasticity modulus were 113.99 MPa, 239.07 MPa, and 17.39 GPa, which were 97.56%, 64.07%, and 66.09% higher than those of moso bamboo (*Phyllostachys edulis*), respectively. The compressive strength, flexural strengths, and elasticity modulus of *B. arundinaceae* were positively correlated with both the distribution density of VBs and the volume fraction of FSs. These insights are crucial for the advancement of durable and efficient materials in diverse sectors including construction and manufacturing.



**Citation:** Zhang, K.; Yu, L.; Dai, F.; Chen, Y.; Jiang, Z.; Wang, Y.; Tian, G. Bamboo Structure and Its Impact on Mechanical Properties: A Case Study of *Bambusa arundinaceae*. *Forests* **2024**, *15*, 762. <https://doi.org/10.3390/f15050762>

Academic Editor: André Luis Christoforo

Received: 1 April 2024

Revised: 22 April 2024

Accepted: 23 April 2024

Published: 26 April 2024



**Copyright:** © 2024 by the authors. Licensee MDPI, Basel, Switzerland. This article is an open access article distributed under the terms and conditions of the Creative Commons Attribution (CC BY) license (<https://creativecommons.org/licenses/by/4.0/>).

## 1. Introduction

Bamboo belongs to the family Gramineae. According to statistics, there are over 1640 species of bamboo plants belonging to 123 genera globally, mainly in the tropics and subtropics [1,2]. As a biodegradable and renewable resource, bamboo matures in 3–5 years. Depending on the growing environment, the maximum growth rate can be up to 100 cm/d [3]. Research has shown that the high carbon sequestration capacity of bamboo can help mitigate climate change. The mechanical properties of bamboo are comparable to those of wood. Particularly, the hardness of some bamboo species is even comparable to that of hardwood. Obataya et al. [4] investigated the mechanical properties of moso bamboo (*Phyllostachys edulis*) through cyclic bending tests and found that, while bamboo exhibited limited elasticity, it demonstrates remarkable ductility. Notably, at comparable densities, the flexural ductility of bamboo surpasses that of wood by a factor of 3.06. Furthermore, while the elasticity modulus of bamboo is 0.84 times that of wood, its flexural strength of bamboo is 1.72 times greater than wood [5]. However, bamboo has some limitations. It is susceptible to cracking and vulnerable to attacks by insects and fungi [6,7]. Additionally, the collection of moso bamboo and the reduction of transportation costs pose challenges due to the geographical areas where it grows.

Among many natural materials, bamboo is a material with a gradient structure and a wealth of advantages [8]. This hollow, rattan-like structure contributes to its distinctive mechanical properties. The excellent bending properties allow it to withstand wind and snow without damage [9], a characteristic that ancient engineers discovered and exploited early on. For example, in South America, the traditional building technique called Quincha, which involves interweaving pieces of wood, rattan, or bamboo into a frame, dates back at least 8000 years [10]. Nowadays, the excellent mechanical properties and eco-friendliness of bamboo make it a good material for scaffolding production in places like China [11]. In Indonesia and Vietnam, bamboo is utilized in constructing infrastructure such as churches or bridges [12]. Additionally, bamboo can be burned to produce bamboo charcoal, adsorbing harmful gases and heavy metal ions from solutions, and enhancing the properties of polylactic acid (PLA) [13–16]. In other areas, helically winding bamboo composite pipes are anticipated to supplant plastic and concrete pipes in modernized underground water distribution networks, serving as novel conduits for liquid conveyance [17]. Furthermore, the superior toughness of bamboo composites renders them suitable for the construction of wind turbine blades [18].

The anatomical structure of bamboo affects its mechanical properties, which in turn influence its applications. The vascular bundles within the culm wall are the most crucial factor influencing the properties of bamboo. Therefore, it is necessary to test the mechanical properties of bamboo and observe the connection with the structure. However, most of the observations on the connection between the mechanical properties and structure of bamboo have been focused on moso bamboo.

*Bambusa arundinaceae* is a bamboo species native to India. It is widely cultivated in regions such as Guangzhou and Hong Kong, China [19]. It has a pole height of 10–17 m, diameter of 6–9 cm, internode length of 10–23 cm, and wall thickness of 1–1.5 cm. It is thick and solid with the potential to be a good building material. However, in recent years, research on *B. arundinaceae* has been mainly focused on the medical field [20–22], with less research on its mechanical properties and distribution patterns of vascular bundles. The absence of essential engineering data poses a challenge that must be addressed to utilize this particular species of bamboo as a structural or construction material.

In this study, *B. arundinaceae* was examined to investigate its potential as a building material. This research aimed to analyze the changes in the volume fraction of the fiber sheaths (FSs) and the distribution density of vascular bundles (VBs) along the axial direction. Additionally, the mechanical properties at different heights of bamboo was measured to investigate the relationship between the structure and mechanical performance.

## 2. Materials and Methods

### 2.1. Sample Preparation

Three-year-old *B. arundinaceae* was randomly collected from a bamboo garden in Zhangzhou City, Fujian Province, China, in a subtropical monsoon climate. (Bamboo reaches maturity and exhibits stable characteristics after about three years of growth). The bamboos were cut into 1.5-m-long segments along the axial direction, totaling 10 sections. These segments were numbered from the base to the top as 1, 2, 3, 4, 5, ..., 10. Samples for bending and compression tests were prepared according to GB/T 15780-1995 [23]. A total of 109 samples were used in the compression test and 130 samples were used in the three-point bending test.

### 2.2. Cross-Sectional Scanning of the Sample

The moisture content of the specimen is controlled to 12% by a temperature Humidity Test Chamber (HSW-1000, Saifu, Ningbo, Shanghai, China). The samples for tests were sanded with 320-grade sandpaper (NO28976 from PROXXON, Föhren, Germany). According to GB/T 15780-1995 [23], the sample sizes for the axial compression test after sanding were 20 mm (L, longitudinal), 20 mm (T, tangential), and t mm (R, radial, culm wall thickness), and for the three-point bending test, the sample size was 160 mm × 10 mm × t mm (bamboo wall

thickness). The samples were placed into a scanner (PERFECTION V850 PRO, EPSON, Suwa City, Japan) with a grayscale of 16 degrees and a resolution of 9600 dpi. The total area of the FSs of the sample was identified by the trained YOLO\_V3 model. The volume fraction of the FSs and the tissue ratio were calculated by using Equation (1):

$$V_{vb} = A_{vb} = \frac{\sum_{i=1}^N s_i}{S} \quad (1)$$

where  $V_{vb}$  is the volume ratio,  $A_{vb}$  is the area fraction,  $S_i$  is the area of an FS in cross-section and  $S$  is the area of cross-section. Figure 1 shows the process.

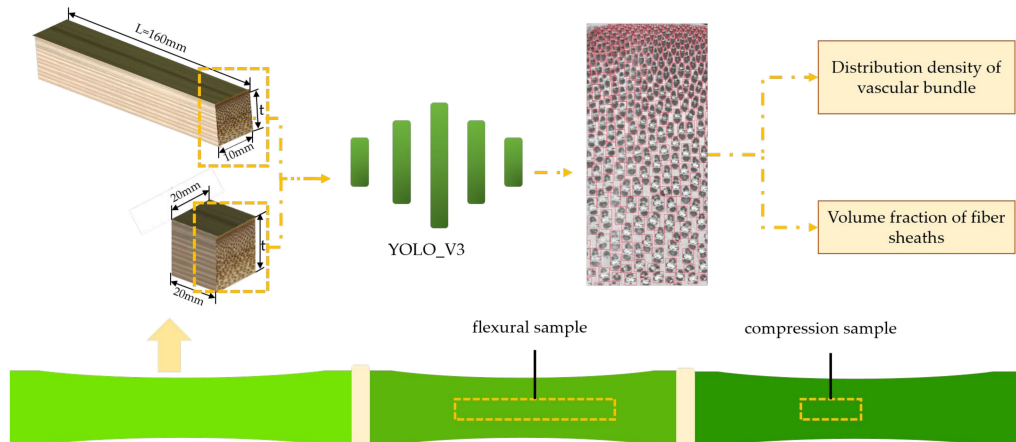


**Figure 1.** Preparation process of samples.

### 2.3. Axial Compression Test

The axial compression test was accomplished by using an Instron Microtester (5848, Instron Co., Norwood, MA, USA). According to the standard of GB/T 15780-1995 [23], the compression rate of the machine was 1.6 mm/min, and the duration of the test was 30 to 90 s. To guarantee the accuracy of the measurement, the machine is equipped with precision sensors and a spherical base that ensures that the top and bottom of the sample fit perfectly into the upper and lower bases during the pressing process (Figure 2). The compressive strength is defined by using Equation (2):

$$\sigma_C = \frac{P}{bt} \quad (2)$$

where  $\sigma_C$  is the axial compressive strength of the sample,  $P$  is the load,  $b$  is the width of the sample, and  $t$  is the thickness of the sample.

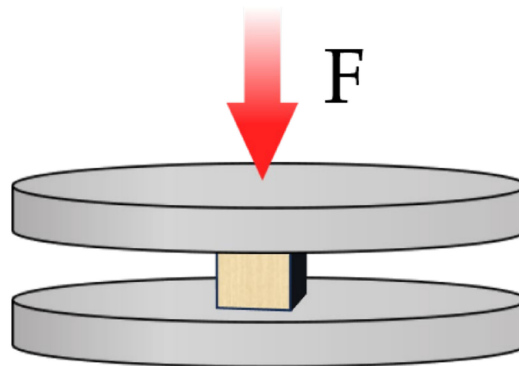


**Figure 2.** Compression experiments.

### 2.4. Three-Point Bending Test

The three-point bending test was accomplished by using an Instron Microtester (5848, Instron Co.). The three-point bending test is tested only in the chordal direction to prevent

the influence of the yellow side and green side on the flexural strength since the distribution of VBs within the culm wall of the bamboo is not uniform. According to the standard of GB/T 15780-1995 [23], the central single-point loading was used, and the sample was placed on two supports of the test device with a span of 120 mm. The load was applied at a uniform rate along the tangential direction of the sample, and the duration of the test was 30 to 90 s (Figure 3). Repeated loading of each sample occurred six times. The initial loading cycle serves to relieve internal stresses within the sample. The subsequent second through fifth cycles aim to calculate the elasticity modulus of the sample, utilizing the average of the three tests. The final cycle determines the flexural strength of the sample (loading until the specimen is destroyed). The flexural strength and elasticity modulus are given by Equations (3) and (4), respectively.

$$\sigma_F = \frac{3PL}{2th^2} \quad (3)$$

$$E = \frac{P_\Delta L^3}{4th^3f} \quad (4)$$

where  $\sigma_F$  is the flexural strength,  $P$  is the load,  $L$  is the span,  $t$  is the thickness of the sample,  $h$  is the height in the chordal direction,  $E$  is the elasticity modulus,  $P_\Delta$  is the difference between the upper-bound and the lower-bound load, and  $f$  is the deformation values at the upper-bound load and lower-bound load.

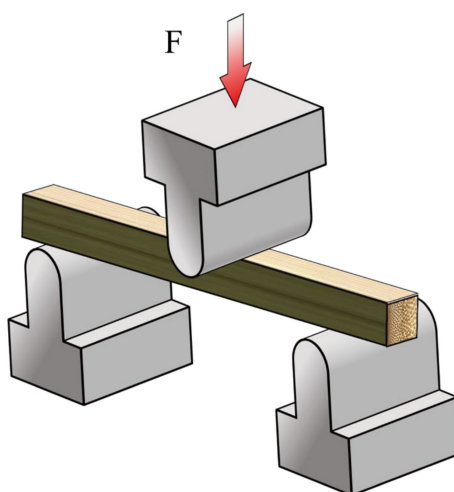


**Figure 3.** Three-point bending test.

### 3. Results

#### 3.1. Structure of Bamboo

The distribution pattern of VBs in bamboo is a direct reflection of its structural characteristics. The distribution density and size of vascular bundles are closely related to the strength, stiffness, and other mechanical properties of bamboo. From a mechanical standpoint, bamboo can be categorized into two components. The first component is the FS, located within VBs. The load-bearing and support structure of bamboo is mostly determined by this part, which allows it to maintain its form and structural integrity. The second component comprises the parenchyma cells (PCs), which function as load-transfer and stress-buffering elements, principally influencing the ductility of bamboo [24]. These two constituents, the FSs and PCs, are the key factors influencing the mechanical properties of bamboo. Consequently, bamboo can be considered a natural composite material. This composite structure gives bamboo both high strength and high toughness, which may explain its use as a structural and building material.

The thickness of the culm wall decreases as the height increases (Figure 4), which is the form in which the bamboo reduces its weight. The VBs near the green side of the bamboo are small, densely packed, poorly differentiated, and mainly composed of fibers;

the VBs in the middle and near the yellow side of the bamboo are larger and sparser, with a stable morphology and well-differentiated transport tissues.

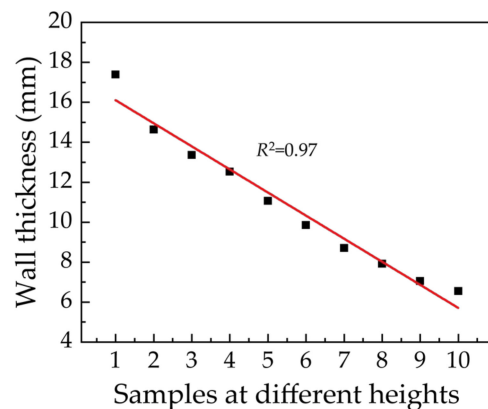


**Figure 4.** Thickness of culm wall at different heights. Note: The X-axis indicates the serial number of the bamboo segments from the base to the top.

The types of VB in bamboo are categorized into five main categories: open, semi-open, broken-waist, double broken-waist, and tight-waist types [25]. The VBs near the green side are small and densely packed with an indistinct differentiation, primarily composed of fibers, and the predominant type is the semi-open type (Figure 5a). The VBs in the middle and towards the yellow side are larger and more sparsely distributed, with a stable morphology and well-differentiated vascular tissues, mainly comprising a mixture of the broken-waisted and a small proportion of the double broken-waisted (Figure 5b,c). These are distributed in the middle and inner regions, with the inner VBs exhibiting a higher degree of differentiation compared to those in the middle.

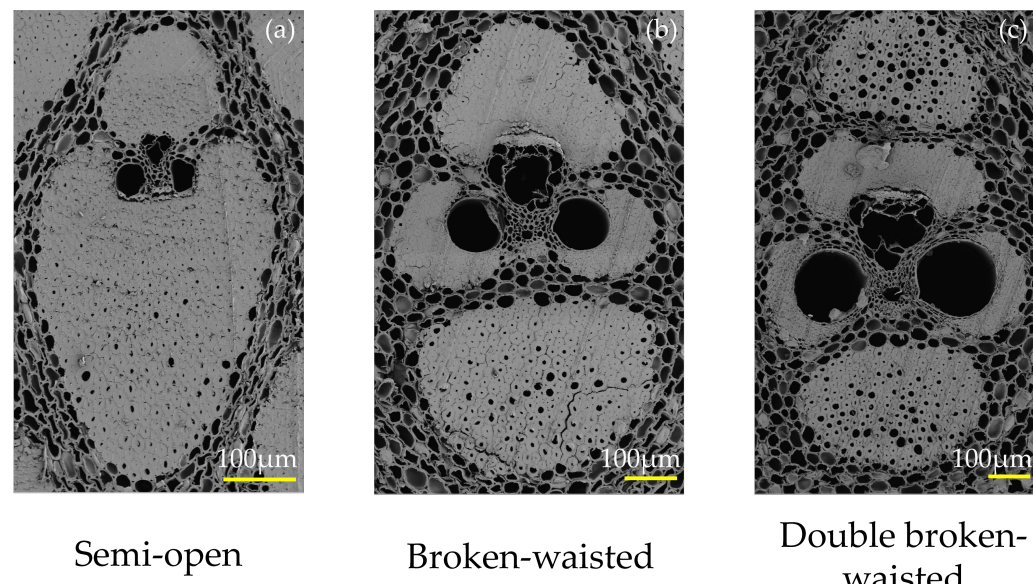


**Figure 5.** Types of VBs. (a) Poorly differentiated VBs (tight-waist type). (b) Broken-waisted type. (c) Double broken-waisted type.

The distribution density of the VBs and the volume fraction of the FSs of the samples showed an overall increasing trend with increasing height, but both decreased in group 4 and then continuously increased, with mean values of 2.91 pcs/mm<sup>2</sup> and 37.7%, respectively (Figure 6a,b). As a result, the distribution of VBs in the radial and axial directions of bamboo is not uniform, which leads to the inhomogeneity of the mechanical properties of bamboo. The distribution density of VBs of *B. arundinaceae* was higher than that of the moso

bamboo ( $2.49 \text{ pcs/mm}^2$ ) [26], and about 1.17 times that of the moso bamboo. Combined with the previous section, it can be hypothesized that the mechanical properties may be superior to those of moso bamboo.

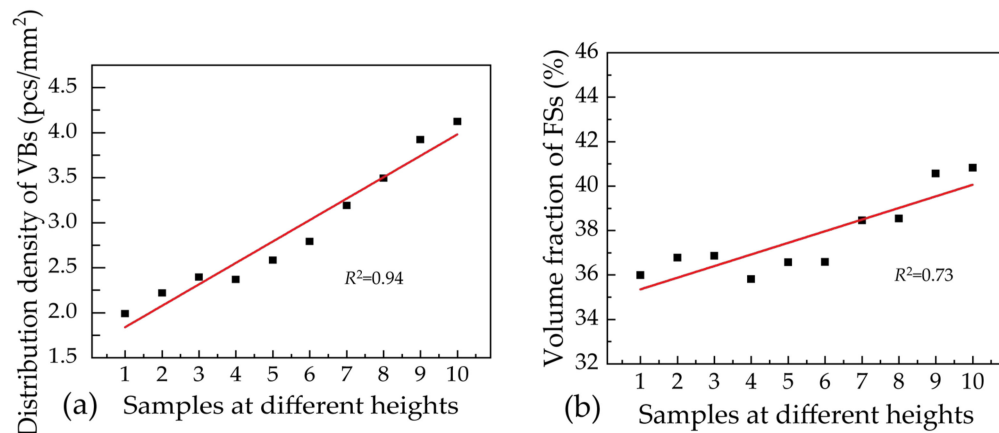


**Figure 6.** Distribution density of VBs (a) volume fraction of FSs (b). Note: The X-axis indicates the serial number of the bamboo segments from the base to the top.

### 3.2. Compression Experiment

#### 3.2.1. Compressive Properties in the Axial Direction

All the samples showed three stages of compression similar to that of laminated bamboo: elastic deformation stage, elastic-plastic stage, and plastic plateau stage [27]. In the elastic deformation stage, the load increases linearly with displacement, and the load at this stage is in the normal range for fibers, which were still able to maintain their original morphology until they reached the proportionality limit. At this stage, PCs with foam-like properties may hinder the lateral deformation of the fibers, allowing the fibers to perform better in the compression process [28]. After reaching the proportional limit, the sample enters the elastic-plastic stage. During this stage, the fibers begin to yield, and although the load continues to increase with displacement, the rate of increase gradually decreases until it becomes zero. The sample then enters the plastic plateau stage. At this point, the load decreases with increasing displacement, but the duration of this stage is much longer than the previous two stages. The prolonged plastic plateau period may be attributed to the PCs being able to absorb larger compressive deformations, increasing the time required for the bamboo to reach failure [29].

As previously stated, the FSs within VBs have a crucial role in providing support and bearing loads, making them the primary component that influences the mechanical properties of bamboo. The compressive strength of bamboo is positively correlated with the distribution density of VBs, which gradually increases from the base to the top along the axial direction. Consequently, the compressive strength also gradually increases from the base to the top along the axial direction (Figures 7 and 8a). The average compressive strength of *B. arundinaceae* was 113.99 MPa, which is twice that of moso bamboo (57.7 MPa), and even higher than that of *Dendrocalamus sinicus* (92.56 MPa), the world's largest bamboo [30,31]. Samples taken from the lower region of the bamboo exhibited a lower distribution density of VBs, yet exhibited a higher content of PCs and possessed thicker walls. As mentioned earlier, PCs have foam-like properties that prevent lateral deformation of the fibers during compression, so the stiffness of the FSs located within the VBs can be more fully utilized. At the same time, the wall thickness of the samples decreased gradually from the base to the top in the radial direction, while the width and height of all samples remained consistent. This leads to a gradual decrease in the cross-sectional area and the content of PCs of the samples from the base to the top in the axial direction, which in turn leads to a gradual weakening of the effect of transmitting load and preventing transverse deformation of the fibers and a gradual increase in the load per unit

area. As a result, the maximum load that can be carried by the sample decreases from the base to the top in the axial direction (Figure 8b).

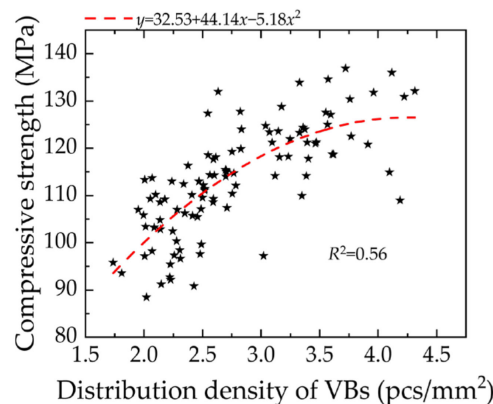


**Figure 7.** The relationship between compressive strength and volume fraction of FSs.

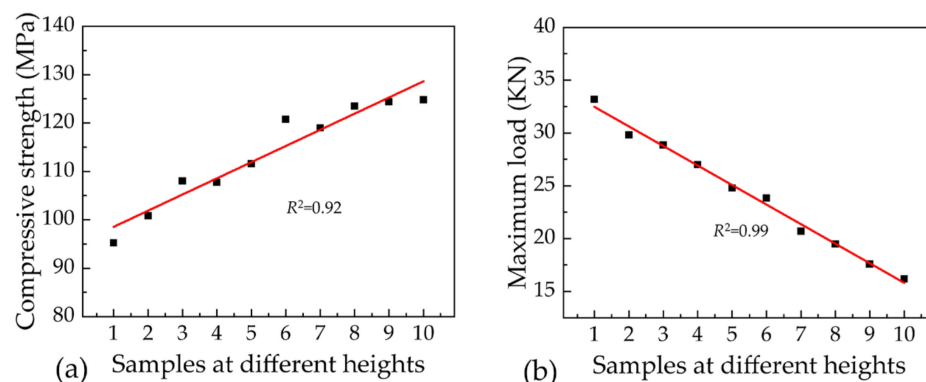


**Figure 8.** Compressive strength (a) and maximum load (b) of samples at different heights. Note: The X-axis indicates the serial number of the bamboo segments from the base to the top.

These findings indicate that as the sample height increased, both the volume fraction and distribution density of the FSs in the bamboo increased progressively. Additionally, the compressive strength of the bamboo increased, but its maximum load capacity declined. These trends may be related to changes in the gradient structure of bamboo VBs. Wall thickness decreases with increasing sampling height, which may lead to a tighter fiber arrangement, thus increasing the compressive strength and stiffness of the bamboo, but at the same time decreasing its load carrying capacity at higher loads. These findings have important implications for understanding and utilizing the structural properties of bamboo, especially for applications in construction and manufacturing.

### 3.2.2. Formatting of Mathematical Components

Compression failure in the axial direction typically arises from the rotational movement of fibers that are locally misaligned. This rotational movement causes shearing of the matrix, resulting in a decrease in its shear modulus. Consequently, the fibers continue to rotate, eventually leading to the breaking of the fibers [32].

In order to study the types of failure of the samples under axial compression and to understand the failure mechanism, each sample was observed and categorized into I to III based on the damage pattern. The crack in type I approximates letter "Y" (Figure 9(a1,a2)). The fibers break during the compression process, which in turn leads to the formation of cracks on the outer surface of the sample. During compression, the crack first appeared in the center of the sample, and as the load increased, the crack gradually expanded towards the two lateral edges in a direction parallel to the 45° folding angle, while the crack in

the center expanded downwards, eventually forming a crack similar to the letter “Y”. A small portion of the sample side appears to expand outward, with the most pronounced expansion at the contact point with the “Y” crack side (Figure 9(b1,b2)). There was no significant change in the sample from the top surface.

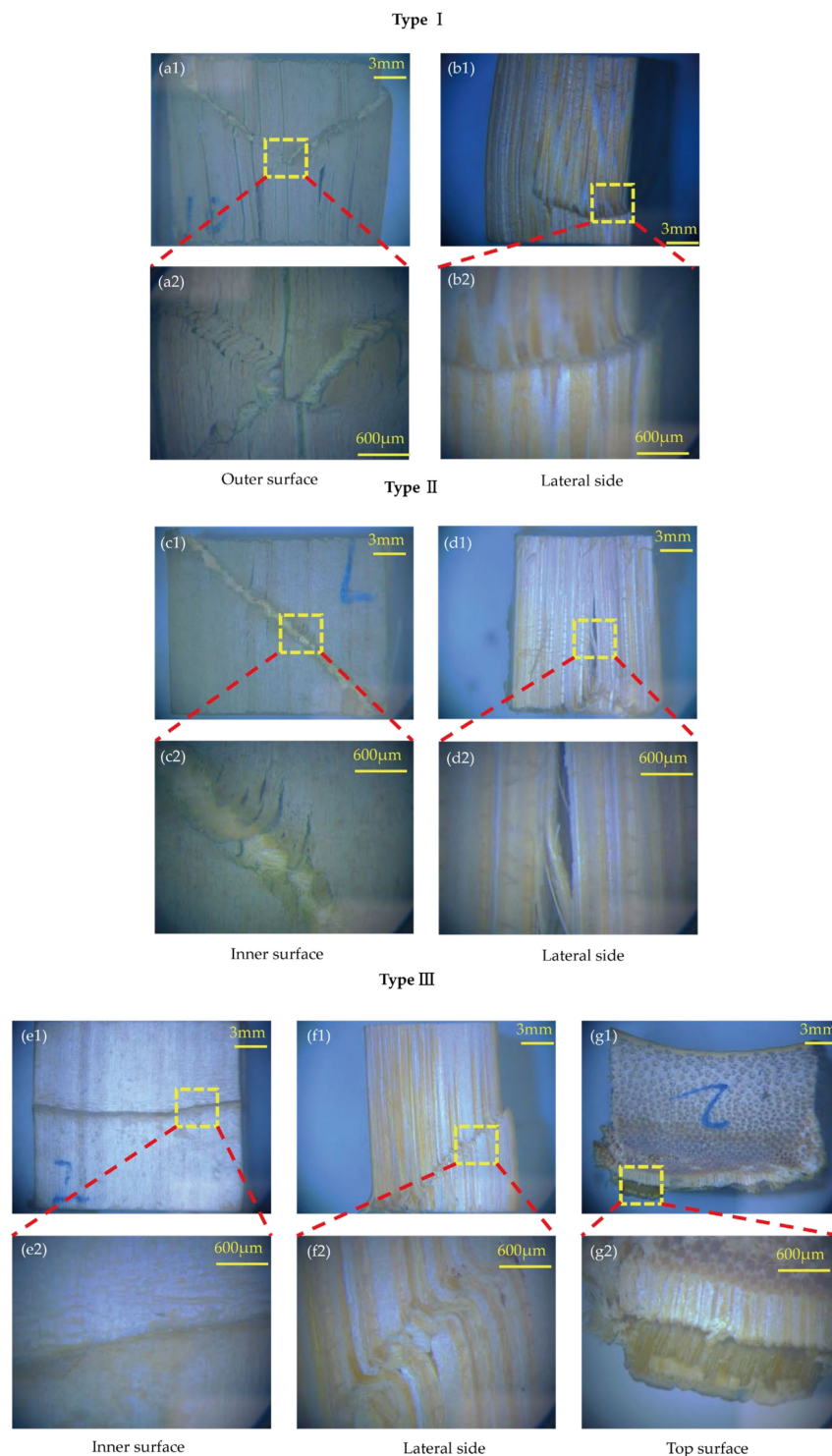


**Figure 9.** Three types of failure. (a1,a2) Outer surface of Type I. (b1,b2) Lateral Side of Type I. (c1,c2) Outer surface of Type II. (d1,d2) Lateral Side of Type II. (e1,e2) Inner surface of type III. (f1,f2) Lateral Side of Type III. (g1,g2) Top surface of Type III.

In type II, the crack expands in a direction of  $45^\circ$  to the loading axis, and as in type I folds and protrusions appear on the outer skin (Figure 9(c1,c2)). This is mainly due to

the bending and misalignment of the fibers during compression, whereas the PCs, due to their characteristics, do not show large cracks during compression [33]. Large cracks were produced on the side of the sample, which may be due to the presence of a weak interface between the fibers and the parenchymal cells and hence the separation. Additionally, fine fiber filaments were observed. As mentioned earlier, bamboo can be classified into two distinct components, the FSs and the PCs, where the FSs are a whole unit formed by the aggregation of many bamboo fibers, which suggests that the FSs were unable to withstand the excessive load during the compression process and thus segregated (Figure 9(d1,d2)).

Unlike types I and II, the outer epidermis of type III is generally little changed, but about 50% of the inner epidermis bulges outward (Figure 9(e1,e2)). From the top surface, the outer epidermis appears to be separated from the stroma. A crack at an angle of 45° to the loading axis can be observed on the lateral side of the sample, identical to that in Type II, which is also caused by fiber bending and misalignment (Figure 9(f1,f2)). The trace of the crack spreads from one apex of the side to the other side and finally reaches the midpoint of that side. As a result, the fibers gradually break in a direction 45° to the loading axis rather than in a direction parallel to the diagonal of the flank, which in turn forms a shear band. From the top surface of the sample, the separation of the matrix and the outer epidermis of the sample occurred during compression. This may be due to the fact that the fibers within the matrix exert a force on the outer epidermis in a horizontal aspect after bending and misalignment, and the degree of separation increases with increasing load (Figure 9(g1,g2)).

Overall, all samples broadly exhibited the three failure types described above, all three of which were shear damage. Gaining insight into the method by which bamboo is destroyed under compression can enhance the efficiency of utilizing bamboo and enable the identification of suitable applications for different parts of bamboo based on their structural needs.

### 3.3. Bending Experiment

#### 3.3.1. Flexural Properties

There was a favorable correlation between the distribution density of VBs and both the flexural strength and elasticity modulus of bamboo. (Figure 10d,e). The flexural strength increased from 209.93 MPa in group 1 to 256.21 MPa in group 6, showing an increasing trend (Figure 10a). This may be related to the reduction of wall thickness and the change in the internal structure of bamboo. The elasticity modulus increased from 15.44 GPa in group 1 to 19.09 GPa in group 6, and the rigidity of bamboo increased with the decrease in wall thickness (Figure 10b). The maximum load exhibited a declining tendency as the group size increased, and a reduction in wall thickness resulted in a substantial decrease in the capacity to bear loads. (Figure 10c).

In the process of increasing from group 6 to group 10, the flexural strength fluctuated greatly, with an average value of 256.62 MPa, which first slightly increased and then decreased, but then slightly recovered in group 10, which may reflect that the internal structure of bamboo becomes more compact with the decrease of wall thickness (Figure 10b). The maximum load still showed a gradually decreasing trend, starting from an average of 1118.44 N in group 6, which indicated that the overall load-carrying capacity of the bamboo material was still decreasing with the decrease in wall thickness (Figure 10c). The modulus of elasticity showed an overall fluctuating trend with an average value of 18.53 GPa, which first decreased and then recovered in group 10, indicating that the rigidity of bamboo is changing with the reduction of wall thickness (Figure 10a). These data indicate that the performance characteristics of bamboo, such as flexural strength and elasticity modulus, show some fluctuation as the wall thickness decreases, but overall show a certain upward trend. Nevertheless, the reduction in load-carrying capacity implies the necessity of evaluating the impact of wall thickness on the performance of bamboo in various applications. In addition, the average flexural strength and flexural elasticity modulus of *B. arundinaceae* were 239.07 MPa and 17.39 GPa, which were 64.07% and 66.09%

higher than those of moso bamboo, respectively. This indicates that *B. arundinaceae* has a better load-bearing capacity than moso bamboo [5].

Overall, *B. arundinaceae* exhibited changes in flexural strength, elasticity modulus, and maximum load when subjected to the bending test for the same reasons that the samples subjected to a compression test may have.

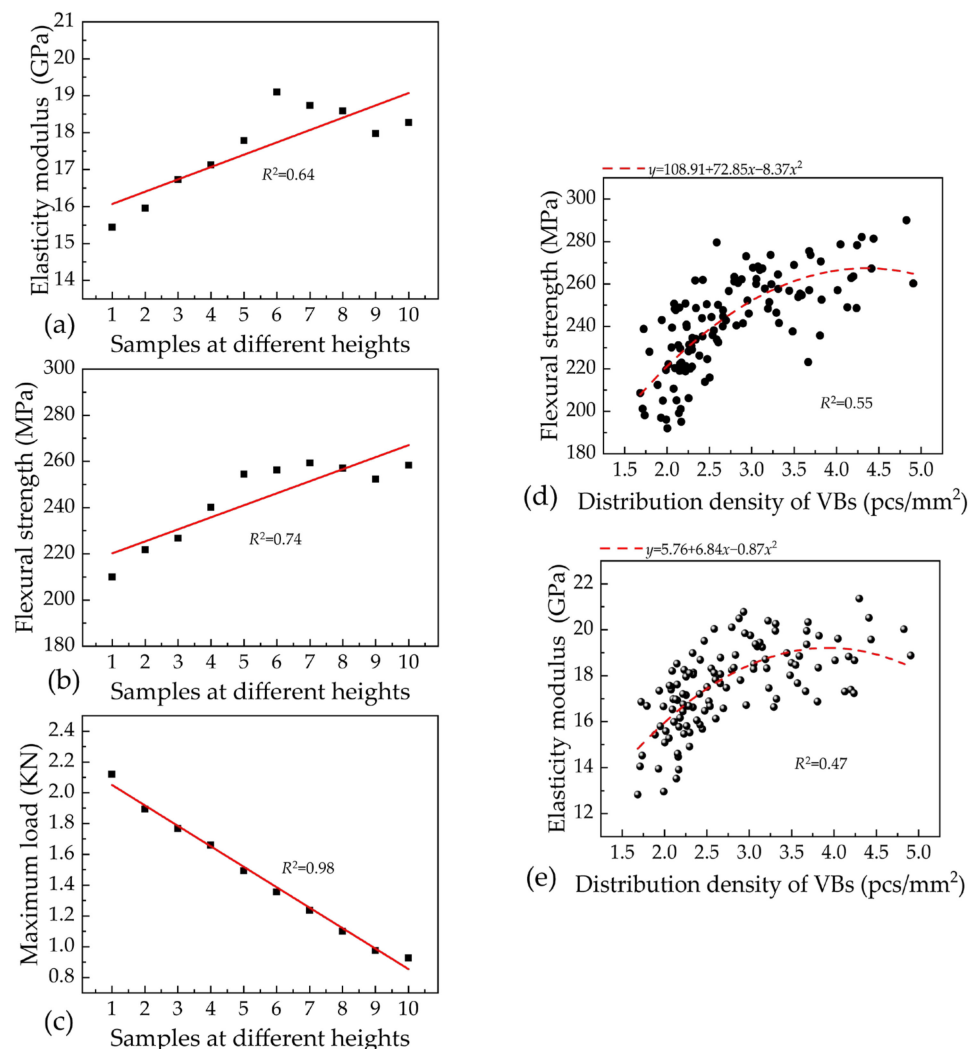


**Figure 10.** Elasticity modulus at different heights (a). Flexural strength at different heights (b). Maximum load at different heights (c). Relationship between distribution density of VBs and flexural strength (d). Relationship between distribution density of VBs and elasticity modulus (e). Note: X-axis indicates the number of bamboo segments from the base to the top.

### 3.3.2. Flexural Behavior of Bamboo Blocks

Although the samples were subjected to top-down pressure in the chordal direction, the bamboo strips exhibited similar destructive characteristics to those subjected to pressure from the radial direction. Since the high-strength fibers are mainly located on the green side and the more ductile PCs are mainly concentrated on the yellow side, the two sites showed different forms of failure (Figure 11).

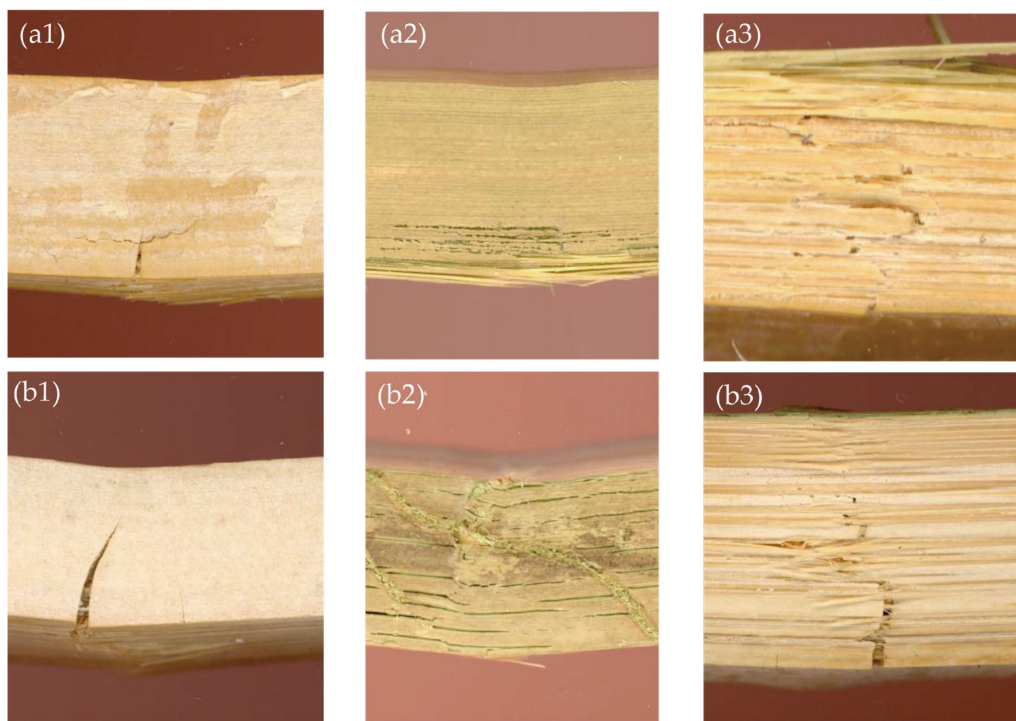


**Figure 11.** The density distribution of VBs was higher on the yellow side (a1), green side (a2), and bottom side (a3) of the samples. The density distribution of VBs was lower on the yellow side (b1), green side (b2), and bottom side (b3) of the samples.

In the contact area with the fixture, the sample with a higher density of VBs did not undergo a large morphological change on the green side, but the yellow side of the sample was wrinkled. The side of the sample that was not in touch with the fixture maintained a perpendicular orientation to the loading axis. Numerous cracks, extending in the axial direction, were observed on this side. Furthermore, the cracks that were located closer to the bottom side of the sample had a greater length (Figure 11(a2)). The event of the appearance of cracks in the axial direction is gradual and progressive, and each appearance means that the overall load-bearing capacity of the sample decreases once. The fibers within the VBs have strong stiffness, while the PCs are ductile but have poor mechanical properties. Due to the tensile force, the shear stress reached the interface strength [34] between the fibers and the PCs, and the chemical bond at the interface broke, which in turn led to the separation of the fibers and the PCs from each other in the green side of the bamboo. At the same time, the fibers could not withstand the excessive tensile force and broke, and eventually there were several axial cracks of different lengths on the green side of the bamboo. On the other hand, on the yellow side of the bamboo, the content of fibers is smaller than the content of PCs, which means that under overloading, the fibers and PCs on the yellow side of the bamboo will break off directly, but will not separate or will separate to a lesser extent (Figure 11(a1)). In addition, fiber breakage and pull-off were more visualized on the bottom side of the specimen, and the extent of breakage and pull-off was greater near the green side of the bamboo (Figure 11(a3)).

The samples with a lower density of VBs exhibited comparable failure characteristics to the samples with a higher density of VBs. However, the axial cracks on the green side were longer and more abundant, while the tangential cracks on the yellow side were also longer (Figure 11(b1–b3)). At the same time, some samples showed splitting.

The gradient structure due to the gradient distribution of VBs is the direct cause of the different failure behavior observed between the green side and yellow side of bamboo. Meanwhile, the interfacial strength also affects the failure type of bamboo and the maximum load it can withstand. This indicates that methods aimed at improving the

interfacial strength of bamboo could potentially enhance its overall mechanical properties. However, the interfacial strength is only one factor influencing the mechanics of bamboo, and improving its mechanical properties necessitates a multifaceted approach, such as enhancing the strength of FSs and PCs. In addition, the rational utilization of bamboo or its different parts, with varying strengths and ductility, according to the actual requirements of structures or buildings, can contribute to waste reduction and cost optimization.

#### 4. Conclusions

The relationship between the structure of *B. arundinaceae* and its mechanical properties was determined through compression and the three-point bending test. The results showed that the compressive strength, flexural strength, and elasticity modulus of *B. arundinaceae* were higher compared to those of moso bamboo. Furthermore, these properties were significantly correlated to the distribution density of VBs. The density of VBs steadily increased from the base to the top along the axial direction. At the same time, the tests also confirmed a corresponding increase in compressive strength, flexural strength, and elasticity model along the axial direction. During axial compression, bamboo had three failure types, all of which are shear damage. However, when exposed to chordal bending, the green and yellow sides of bamboo demonstrate distinct failure types. The disparity is mainly ascribed to the distinct mechanical characteristics of the PCs and VBs in bamboo, as well as their respective composition. *B. arundinaceae* possesses exceptional mechanical characteristics and is anticipated to emerge as a novel and environmentally friendly construction material.

However, as previously mentioned, bamboo has certain limitations that restrict its application. To mitigate these limitations, consider the following methods before using bamboo.

Before use, ensure that the water content in the bamboo is reduced by drying and applying natural or artificial preservatives to protect the bamboo from decay and pests.

Adjust the moisture content within the bamboo to minimize deformation. This adjustment should align with the specific requirements of the building or structure.

**Author Contributions:** Conceptualization, F.D.; data curation, L.Y.; formal analysis, Y.W.; funding acquisition, G.T.; supervision, Z.J.; writing—original draft, K.Z.; writing—review and editing, Y.C. All authors have read and agreed to the published version of the manuscript.

**Funding:** This research was funded by the Basic Scientific Research Funds of International Center for Bamboo and Rattan (Grant number 1632023015), the National Natural Science Foundation (grant no. 32071855), and the National Key R&D Program of China (2022YFD2200901). And The APC was funded by the Basic Scientific Research Funds of International Center for Bamboo and Rattan (Grant number 1632023015).

**Data Availability Statement:** Data will be made available on request.

**Conflicts of Interest:** The authors declare that they have no known competing financial interests or personal relationships that could have appeared to influence the work reported in this paper.

#### References

1. Zhang, Y.; Wu, L.; Li, Y.; Yang, J.; Yang, H.; Zhao, Y.; Chen, G. Bamboo shoot and its food applications in last decade: An undervalued edible resource from forest to feed future people. *Trends Food Sci. Technol.* **2024**, *146*, 104399.
2. Emamverdian, A.; Ding, Y.; Ranaei, F.; Ahmad, Z. Application of bamboo plants in nine aspects. *Sci. World J.* **2020**, *2020*, 7284203.
3. Xu, Y.; Wong, M.; Yang, J.; Ye, Z.; Jiang, P.; Zheng, S. Dynamics of carbon accumulation during the fast growth period of bamboo plant. *Bot. Rev.* **2011**, *77*, 287–295. [[CrossRef](#)]
4. Obataya, E.; Kitin, P.; Yamauchi, H. Bending characteristics of bamboo (*Phyllostachys pubescens*) with respect to its fiber–foam composite structure. *Wood Sci. Technol.* **2007**, *41*, 385–400. [[CrossRef](#)]
5. Chen, M.; Ye, L.; Li, H.; Wang, G.; Chen, Q.; Fang, C.; Dai, C.; Fei, B. Flexural strength and ductility of moso bamboo. *Constr. Build. Mater.* **2020**, *246*, 118418. [[CrossRef](#)]
6. Lv, H.; Lian, C.; Xu, B.; Shu, X.; Yang, J.; Fei, B. Effects of microwave-assisted drying on the drying shrinkage and chemical properties of bamboo stems. *Ind. Crops Prod.* **2022**, *187*, 115547. [[CrossRef](#)]
7. Huang, L.; He, J.; Tian, C.-M.; Li, D.-W. Bambusicolous fungi, diseases, and insect pests of bamboo. *For. Microbiol.* **2023**, *3*, 415–440.

8. Amada, S. Hierarchical functionally gradient structures of bamboo, barley, and corn. *Mrs Bull.* **1995**, *20*, 35–36. [[CrossRef](#)]
9. Wei, X.; Zhou, H.; Chen, F.; Wang, G. Bending flexibility of moso bamboo (*Phyllostachys edulis*) with functionally graded structure. *Materials* **2019**, *12*, 2007. [[CrossRef](#)]
10. Rael, R. *Earth Architecture*; Princeton Architectural Press: New York, NY, USA, 2009.
11. Chung, K.F.; Yu, W. Mechanical properties of structural bamboo for bamboo scaffoldings. *Eng. Struct.* **2002**, *24*, 429–442. [[CrossRef](#)]
12. Xu, H.; Li, J.; She, Y.; Wang, H.; Xu, X. The unique flexibility feature of moso bamboo: Arising implications for biomimetic material design. *Constr. Build. Mater.* **2024**, *411*, 134568. [[CrossRef](#)]
13. Wang, F.Y.; Wang, H.; Ma, J.W. Adsorption of cadmium (II) ions from aqueous solution by a new low-cost adsorbent—Bamboo charcoal. *J. Hazard. Mater.* **2010**, *177*, 300–306. [[CrossRef](#)] [[PubMed](#)]
14. Kandhavadi, P.; Vigneswaran, C.; Ramachandran, T.; Geethamanohari, B. Development of polyester-based bamboo charcoal and lyocell-blended union fabrics for healthcare and hygienic textiles. *J. Ind. Text.* **2011**, *41*, 142–159. [[CrossRef](#)]
15. Ho, M.-p.; Lau, K.-t.; Wang, H.; Hui, D. Improvement on the properties of polylactic acid (PLA) using bamboo charcoal particles. *Compos. Part B Eng.* **2015**, *81*, 14–25. [[CrossRef](#)]
16. Asada, T.; Ishihara, S.; Yamane, T.; Toba, A.; Yamada, A.; Oikawa, K. Science of bamboo charcoal: Study on carbonizing temperature of bamboo charcoal and removal capability of harmful gases. *J. Health Sci.* **2002**, *48*, 473–479. [[CrossRef](#)]
17. Chen, M.; Weng, Y.; Semple, K.; Zhang, S.; Jiang, X.; Ma, J.; Fei, B.; Dai, C. Sustainability and innovation of bamboo winding composite pipe products. *Renew. Sustain. Energy Rev.* **2021**, *144*, 110976. [[CrossRef](#)]
18. Holmes, J.W.; Brøndsted, P.; Sørensen, B.F.; Jiang, Z.; Sun, Z.; Chen, X. Development of a bamboo-based composite as a sustainable green material for wind turbine blades. *Wind Eng.* **2009**, *33*, 197–210. [[CrossRef](#)]
19. Li, J. Flora of China. *Harv. Pap. Bot.* **2007**, *13*, 301–302. [[CrossRef](#)]
20. Iqbal, S.M.; Hussain, L.; Hussain, M.; Akram, H.; Asif, M.; Jamshed, A.; Saleem, A.; Siddique, R. Nephroprotective potential of a standardized extract of bambusa arundinacea: In vitro and in vivo studies. *ACS Omega* **2022**, *7*, 18159–18167. [[CrossRef](#)]
21. Zihad, S.N.K.; Saha, S.; Rony, M.S.; Banu, H.; Uddin, S.J.; Shilpi, J.A.; Grice, I.D. Assessment of the laxative activity of an ethanolic extract of Bambusa arundinacea (Retz.) Willd. shoot. *J. Ethnopharmacol.* **2018**, *214*, 8–12. [[CrossRef](#)]
22. Naradala, J.; Allam, A.; Tumu, V.R.; Rajaboina, R. Antibacterial activity of copper nanoparticles synthesized by Bambusa arundinacea leaves extract. *Biointerface Res. Appl. Chem.* **2021**, *12*, 1230–1236.
23. GB/T 15780-1995; Testing Methods for Physical and Mechanical Properties of Bamboos. The State Bureau of Quality and Technical Supervision: Beijing, China, 1995.
24. Shao, Z.; Wang, F. *The Fracture Mechanics of Plant Materials: Wood and Bamboo*; Springer: Singapore, 2018; pp. 117–134. [[CrossRef](#)]
25. Lian, C.; Liu, R.; Zhang, S.; Luo, J.; Fei, B. Research progress on anatomical structure of bamboo vascular bundles. *China For. Prod. Ind.* **2018**, *45*, 8–12. [[CrossRef](#)]
26. Li, J.; Xu, H.; Yu, Y.; Chen, H.; Yi, W.; Wang, H. Intelligent analysis technology of bamboo structure. Part I: The variability of vascular bundles and fiber sheath area. *Ind. Crops Prod.* **2021**, *174*, 114163. [[CrossRef](#)]
27. Li, H.-t.; Zhang, Q.-s.; Huang, D.-s.; Deeks, A.J. Compressive performance of laminated bamboo. *Compos. Part B Eng.* **2013**, *54*, 319–328. [[CrossRef](#)]
28. Huang, D.S.; Zhou, A.P.; Li, H.T.; Su, Y.; Chen, G. Experimental study on the tensile properties of bamboo related to its distribution of vascular bundles. *Key Eng. Mater.* **2012**, *517*, 112–117. [[CrossRef](#)]
29. Su, Q.; Chen, L.; Dai, C.; Fei, B.; Chen, X.; Luo, X.; Fang, C.; Ma, X.; Zhang, X.; Liu, H. Structure and mechanisms of foam-like bamboo parenchyma tissue. *J. Mater. Res. Technol.* **2023**, *27*, 617–629. [[CrossRef](#)]
30. Dai, F.; Wang, Z.; Wang, H.; Zhang, W.; Zhong, T.; Tian, G. Vascular bundle characteristics and mechanical properties of *Dendrocalamus sinicus*. *Constr. Build. Mater.* **2023**, *363*, 129858. [[CrossRef](#)]
31. Zhou, Q.; Tian, J.; Liu, P.; Zhang, H. Test and prediction of mechanical properties of Moso bamboo. *J. Eng. Fibers Fabr.* **2021**, *16*, 15589250211066802. [[CrossRef](#)]
32. Talreja, R.; Waas, A.M. Concepts and definitions related to mechanical behavior of fiber reinforced composite materials. *Compos. Sci. Technol.* **2022**, *217*, 109081. [[CrossRef](#)]
33. Zhang, X.; Li, J.; Yu, Z.; Yu, Y.; Wang, H. Compressive failure mechanism and buckling analysis of the graded hierarchical bamboo structure. *J. Mater. Sci.* **2017**, *52*, 6999–7007. [[CrossRef](#)]
34. Chen, G.; Luo, H.; Yang, H.; Zhang, T.; Li, S. Water effects on the deformation and fracture behaviors of the multi-scaled cellular fibrous bamboo. *Acta Biomater.* **2018**, *65*, 203–215. [[CrossRef](#)] [[PubMed](#)]

**Disclaimer/Publisher’s Note:** The statements, opinions and data contained in all publications are solely those of the individual author(s) and contributor(s) and not of MDPI and/or the editor(s). MDPI and/or the editor(s) disclaim responsibility for any injury to people or property resulting from any ideas, methods, instructions or products referred to in the content.